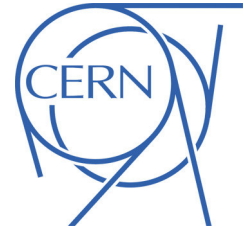




# ATLAS NOTE

ATLAS-CONF-2011-108

November 9, 2011



## Measurement of the top quark pair production cross-section based on a statistical combination of measurements of dilepton and single-lepton final states at $\sqrt{s} = 7$ TeV with the ATLAS detector

The ATLAS Collaboration

### Abstract

We present a measurement of the top quark pair production cross-section based on a statistical combination of measurements using dilepton final states with  $0.70 \text{ fb}^{-1}$  of data and single-lepton final states with  $35 \text{ pb}^{-1}$  of data. The measured cross-section, which is in good agreement with the Standard Model prediction, is:

$$\sigma_{t\bar{t}} = 176 \pm 5 \text{ (stat.)} \pm \frac{13}{10} \text{ (syst.)} \pm 7 \text{ (lumi.) pb.}$$



# 1 Introduction

The measurement of the top-quark pair-production cross-section,  $\sigma_{SM}$ , is one of the key milestones for the early LHC physics program. A precise measurement of  $\sigma_{t\bar{t}}$  allows precision tests of perturbative QCD, whose uncertainties on  $\sigma_{t\bar{t}}$  are now at the level of 10% [1]. In addition,  $t\bar{t}$  production is an important background to the search for the Higgs boson and various searches for physics beyond the Standard Model. New physics may also give rise to additional  $t\bar{t}$  production mechanisms or modification of the top quark decay channels.

The theoretical prediction of the top-quark cross-section is  $\sigma_{t\bar{t}} = 164.6_{-16}^{+11}$  pb, assuming a top-quark mass of 172.5 GeV [3]. Within the Standard Model, top quarks are predicted to decay to a  $W$  boson and a  $b$ -quark nearly 100% of the time, and the decay topologies are determined by the decays of the  $W$  bosons. The single-lepton mode, with a branching ratio of 34.4%, and the dilepton mode, with a branching ratio of 6.5%, give rise to final states with one or two leptons, missing transverse energy and jets, at least two of which have  $b$ -flavor. Only the leptonic decays of the  $W$  to an electron or muon are considered, including the small contributions from  $W \rightarrow \tau \rightarrow e$  and  $W \rightarrow \tau \rightarrow \mu$ .

This note presents a combined measurement of the  $t\bar{t}$  production cross-section at a center-of-mass energy of  $\sqrt{s} = 7$  TeV using single-lepton and dilepton channels. The single-lepton channel used  $35 \text{ pb}^{-1}$  of data taken in 2010 [4] and the dilepton channel used  $0.70 \text{ fb}^{-1}$  of data taken in 2011 [5]. The luminosity estimates for these datasets have uncertainties of 3.4% [6] and 3.7%, respectively. The dilepton channel measurements are based on simple cut-based analyses in the  $\geq 2$  jet bins without  $b$ -tagging, while the single-lepton channel measurements are based on a multivariate discriminant distribution divided into 3, 4, and  $\geq 5$  jet samples using  $b$ -tagging. The results of the five cross-section measurements from the individual channels as well as the dilepton and single-lepton combinations are shown in Table 1. Even though the dilepton analysis does not require  $b$ -tagging, the combination with the single-lepton channel assumes the branching ratio of  $t \rightarrow Wb$  is 100%.

The two sets of analyses share some common sources of systematic uncertainty, which must be treated consistently in order to form a combination. The likelihood function in each of the channels is a function of the signal cross-section  $\sigma_{t\bar{t}}$ , the integrated luminosity  $\mathcal{L}$ , and several nuisance parameters  $\alpha_j$  that parametrize the effect of various sources of systematic uncertainty.

The full five-channel combination was implemented with an approximate method, in which the single-lepton likelihood function was approximated by a multivariate Gaussian with covariance given by the Hessian matrix from MINUIT's HESSE algorithm [7]. When forming the five-channel combined likelihood, constraint terms for systematic uncertainties that are common to the dilepton and single-lepton channels were included only once.

Each measurement was based on the profile likelihood ratio

$$\lambda(\sigma_{t\bar{t}}) = \frac{L(\sigma_{t\bar{t}}, \hat{\mathcal{L}}, \hat{\alpha}_j)}{L(\hat{\sigma}_{t\bar{t}}, \hat{\mathcal{L}}, \hat{\alpha}_j)}, \quad (1)$$

where  $\hat{\sigma}_{t\bar{t}}, \hat{\mathcal{L}}, \hat{\alpha}_j$  denote the maximum likelihood estimate of all the parameters and  $\hat{\mathcal{L}}$  and  $\hat{\alpha}_j$  represent the conditional maximum likelihood estimates of  $\mathcal{L}$  and  $\alpha_j$  holding  $\sigma_{t\bar{t}}$  fixed. The best fit value of the cross-section is simply  $\hat{\sigma}_{t\bar{t}}$  and the 68% confidence interval is derived from the values of  $\sigma_{t\bar{t}}$  which give  $-2 \log \lambda(\sigma_{t\bar{t}}) = 1$ .

## 2 Dilepton combined likelihood function

The likelihood function for each of the dilepton channels is similar, with a single Poisson term for the number of observed events with  $\geq 2$  jets and several Gaussian constraint terms for the nuisance parameters  $\alpha_j$ . The combined likelihood is given by the product of the Poisson terms and a product of the constraint terms

$$L_{ll}(\sigma_{ll}, \mathcal{L}, \alpha_j) = \text{Gaus}(\mathcal{L}_0 | \mathcal{L}, \sigma_{\mathcal{L}}) \prod_{i \in \{ee, \mu\mu, e\mu\}} \text{Pois}(N_i^{\text{obs}} | N_{i, \text{tot}}^{\text{exp}}(\alpha_j)) \prod_{j \in \text{syst}} \text{Gaus}(0 | \alpha_j, 1), \quad (2)$$

where Pois is the Poisson distribution, Gaus is the Gaussian distribution, and the constraint terms on common systematic uncertainties are only included once. The variation in the expected number of events from the signal and each background process was estimated from dedicated studies of each of the systematic effects. The total number of expected events,  $N_{i, \text{tot}}^{\text{exp}}(\alpha_j)$ , is then parametrized via piece-wise linear interpolation in the nuisance parameters  $\alpha_j$  associated with each source of systematic uncertainty using the RooFit/RooStats software package [8, 9]. The profile likelihood ratios for the individual channels as well as the dilepton combination are shown in Fig. 1. The dominant systematic uncertainties for the dilepton analysis are jet energy scale, lepton identification efficiency, fake lepton rates, and modeling of the signal. Because the dilepton analyses do not use  $b$ -tagging, they are not sensitive to those systematic uncertainties. More information on the combination of measurements using dilepton final states can be found in reference [5].

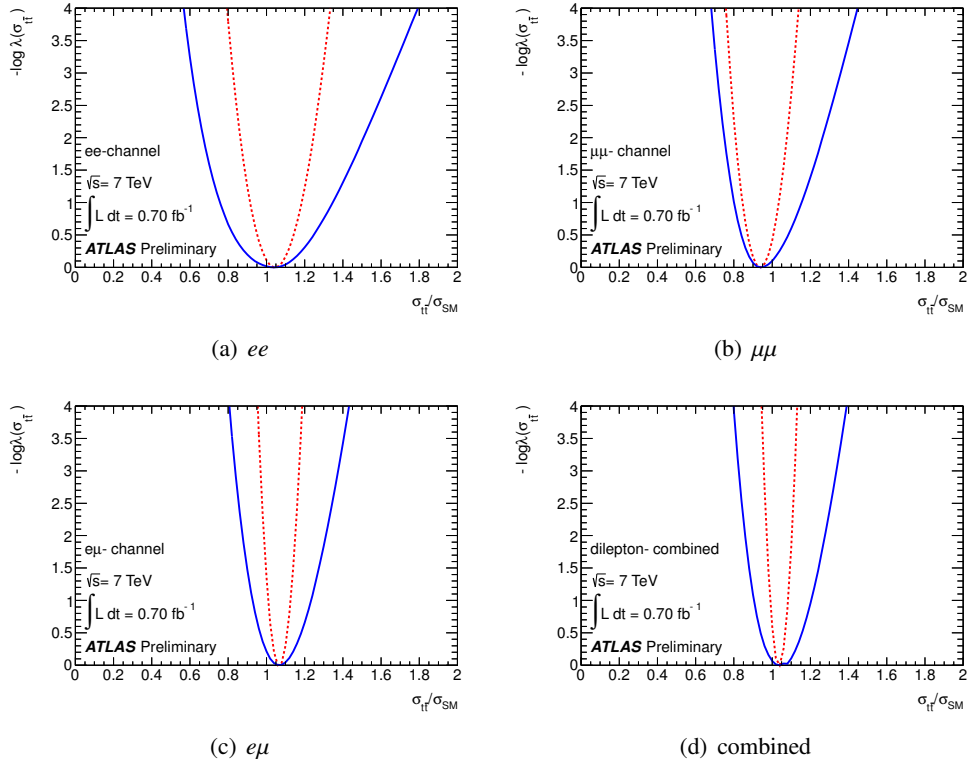


Figure 1: Graphs of  $-\log \lambda(\sigma_{ll})$  vs.  $\sigma_{ll}/\sigma_{\text{SM}}$  with (blue, solid) and without (red, dashed) systematic uncertainties for the individual channels  $ee$  (a),  $\mu\mu$  (b), and  $e\mu$  (c), and the three-channel combined fit (d).

### 3 Approximating the single-lepton likelihood function

The likelihood function for the single-lepton channels is formed from the  $e$ +jets and  $\mu$ +jets models, taking into account common systematic uncertainties. The single-lepton analysis uses continuous  $b$ -tagging: one of the input variables to the likelihood discriminant used in the template fit is the light-flavor probability as obtained from the JetProb  $b$ -tagging algorithm [10]. The uncertainties in the  $b$ -tagging and mistag rates are included as nuisance parameters in the fit. More information on the combination of measurements using single-lepton final states can be found in reference [4]. The likelihood function consists of the parameter of interest,  $\sigma_{i\bar{i}}$ , and 37 nuisance parameters  $\vec{\alpha}$ , which are together denoted  $\vec{\theta} = (\sigma_{i\bar{i}}, \vec{\alpha})$ . The maximum likelihood estimator of this two-channel single-lepton combination is denoted  $\hat{\vec{\theta}}$ .

For the purposes of the five-channel combination, the likelihood from the single-lepton channels was approximated with a multivariate Gaussian. This approximation facilitated the combination with the dilepton likelihood, which was implemented in a different software framework. Figure 2 shows a plot of  $-\log \lambda(\sigma_{i\bar{i}})$  vs.  $\sigma_{i\bar{i}}/\sigma_{SM}$ , where it can be seen that the likelihood is very symmetric and parabolic, indicating that a multivariate Gaussian is a good approximation to the likelihood function. The covariance matrix comes from the Hessian matrix of the negative-log-likelihood function evaluated at the best fit point,

$$V_{ij}^{-1} = -\frac{\partial^2}{\partial\theta_i\partial\theta_j} \log L(\vec{\theta}) \Big|_{\hat{\vec{\theta}}}. \quad (3)$$

With the covariance matrix, one can construct the multivariate Gaussian

$$L_{l+jets}(\vec{\theta}) = G(\hat{\vec{\theta}}|\vec{\theta}, V) = \frac{1}{(2\pi)^{k/2}|V|^{1/2}} \exp\left(-\frac{1}{2}(\hat{\vec{\theta}} - \vec{\theta})^T V^{-1}(\hat{\vec{\theta}} - \vec{\theta})\right), \quad (4)$$

where  $k = 38$  is the dimensionality of the parameter space.

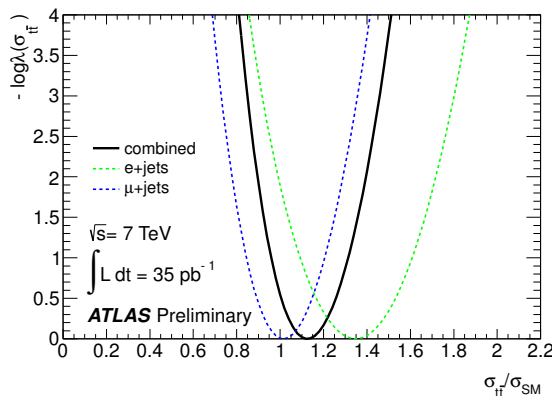


Figure 2: Plot of  $-\log \lambda(\sigma_{i\bar{i}})$  vs.  $\sigma_{i\bar{i}}/\sigma_{SM}$  from the full  $e$ +jets (green, dashed),  $\mu$ +jets (blue, dashed), and  $l$ +jets combined likelihood (black, solid).

## 4 Five-channel combined likelihood function

The dilepton and single-lepton channels share several common sources of systematic uncertainty:

- electron and muon identification uncertainties,
- electron energy scale and resolution uncertainties,
- muon momentum scale and resolution uncertainties,
- Monte Carlo generator, initial state radiation (ISR), and final state radiation (FSR) dependence on acceptance,
- jet energy resolution, jet energy scale, and jet efficiency uncertainties,
- cross-section uncertainties for diboson and single top backgrounds,
- integrated luminosity.

Because the likelihood function from the single-lepton analysis is approximated by a single multivariate Gaussian, the constraint terms that are common with the dilepton channel must be removed when forming the five-channel combination. Before combining, the dependence of the conditional maximum likelihood estimates,  $\hat{\alpha}_j$ , as a function of  $\sigma_{\bar{t}\bar{t}}/\sigma_{SM}$  were compared for the dilepton and single-lepton channels. Those studies did not indicate any unexpected tension in the shared nuisance parameters that would indicate incompatible results.

The final five-channel likelihood (equation 5) is formed from a product of the approximate single-lepton likelihood,  $L_{l+jets}$ , over the parameter of interest,  $\sigma_{\bar{t}\bar{t}}$ , and 37 nuisance parameters (15 of which are shared with the dilepton channels, including a luminosity constraint), the Poisson terms corresponding to the cut-based analyses for the dileptons (which depend on the parameter of interest), and Gaussian constraints for the remaining 31 nuisance parameters that only affect the dilepton channels. We take sources of systematic uncertainty which are shared between channels to be fully correlated. This approach is conservative and we expect differences due to varying data conditions to be small. We assume a common source of systematic uncertainty for the 2010 and 2011 integrated luminosity measurements. In total, there are 69 parameters in the five-channel combined fit.

$$L_{5chan}(\sigma_{\bar{t}\bar{t}}, \mathcal{L}, \alpha_j) = L_{l+jets}(\sigma_{\bar{t}\bar{t}}, \mathcal{L}, \alpha_j) \times \text{Gaus}(\mathcal{L}_0 | \mathcal{L}, \sigma_{\mathcal{L}}) \prod_{i \in \{ee, \mu\mu, e\mu\}} \text{Pois}(N_i^{\text{obs}} | N_{i,\text{tot}}^{\text{exp}}) \prod_{j \in \text{all only sys}} \text{Gaus}(0 | \alpha_j, 1). \quad (5)$$

## 5 Results and conclusions

The result of fitting this combined model to the observed data is summarized in Table 1, together with the five input measurements. The measured value of  $\hat{\sigma}_{\bar{t}\bar{t}}$  is  $176 \pm_{13}^{16}$  pb, with the 68% confidence interval inferred from the asymptotic properties of the profile likelihood ratio, which is shown in Fig. 3. This interval includes the effect of all systematic and statistical uncertainties, including their correlated effects on the signal and backgrounds in the five channels. The statistical uncertainty is obtained by fixing all the nuisance parameters associated with underlying sources of systematic uncertainty to their best fit values. The component of the total uncertainty attributed to the effect of systematic uncertainty is obtained by subtracting in quadrature the statistical contribution from the uncertainty obtained by including all sources of systematic uncertainty except for the luminosity uncertainty. Finally, the uncertainty attributed to the luminosity is obtained by subtracting in quadrature the combined systematic and statistical uncertainties from the total uncertainty, ensuring that the quadratic sum of all three components is consistent with the uncertainty from all contributions.

Channel	$\sigma_{\bar{t}\bar{t}}$ (pb)
$ee$	$172 \pm 16(\text{stat.}) \pm_{33}^{30}(\text{syst.}) \pm_7^8(\text{lumi.})$
$\mu\mu$	$154 \pm 10(\text{stat.}) \pm_{10}^{19}(\text{syst.}) \pm_6^7(\text{lumi.})$
$e\mu$	$176 \pm 7(\text{stat.}) \pm_{14}^{17}(\text{syst.}) \pm 8(\text{lumi.})$
Dilepton combined	$171 \pm 6(\text{stat.}) \pm_{14}^{16}(\text{syst.}) \pm 8(\text{lumi.})$
$e$ +jets	$223 \pm 17(\text{stat.}) \pm 27(\text{syst.}) \pm 8(\text{lumi.})$
$\mu$ +jets	$168 \pm 12(\text{stat.}) \pm_{18}^{20}(\text{syst.}) \pm 6(\text{lumi.})$
Single lepton combined	$186 \pm 10(\text{stat.}) \pm_{20}^{21}(\text{syst.}) \pm 6(\text{lumi.})$
Five-channel combined	$176 \pm 5(\text{stat.}) \pm_{10}^{13}(\text{syst.}) \pm 7(\text{lumi.})$

Table 1: Measured values of  $\sigma_{\bar{t}\bar{t}}$  in each of the five individual analyses, the dilepton and single-lepton combinations, and the full five-channel combination.

The combined cross-section and its statistical uncertainty are in good agreement with a simple approximate calculation in which  $\sigma_{\bar{t}\bar{t}}$  is estimated by a weighted sum based on the inverse of the error of the dilepton and single-lepton results. The total systematic uncertainty is only slightly larger than one would expect for fully uncorrelated uncertainties. While 54 of the 69 uncertainties are in fact uncorrelated between the single-lepton and dilepton models, including several of the larger individual uncertainties such as  $W$ +jets heavy flavor composition and  $b$ -tagging efficiency, the remaining 15 systematic uncertainties are properly treated as correlated. However several of these correlated terms can be effectively constrained from data using the profile likelihood technique and the magnitude of these in the combination is smaller than that in the individual channels as more data is available in the combination to constrain them.

The dominant systematic uncertainties in the five-channel combination, which include  $W$ +jets heavy

Uncertainty source	Uncertainty (pb)
Heavy flavor	4.1
Jet energy scale	3.9
Fake lepton estimate	3.2
Initial and final state radiation	3.0
$b$ -tagging	2.8
Event generator	2.3
Electron efficiency	2.0
Muon efficiency	1.5
W Shape	0.5
QCD Shape	0.4
All others	5.1

Table 2: Dominant sources of systematic uncertainty in the combined five channel model and their contribution to the error on the measured cross section.

flavor content, the dilepton fake lepton background estimate, reconstructed jet identification efficiency, jet energy scale, and initial and final state radiation, are listed in Table 2. The fact that the dilepton analysis does not use  $b$ -tagging serves to reduce the magnitude of the correlation coefficients between  $\sigma_{t\bar{t}}$  and the nuisance parameters related to  $b$ -tagging and the heavy flavor content of  $W$ +jets, thus reducing the total systematic uncertainty slightly.

Figure 4 shows various cross-section measurements from Tevatron and LHC experiments overlaid on the theoretical predictions as a function of center-of-mass energy [11]. The measurement presented in this note, which has a total error of 8.2%, is approaching the precision of recent Tevatron cross-section combinations, which measure  $7.50 \pm 0.48$  pb at  $\sqrt{s} = 1.96$  TeV for an error of 6.4% [12]. Figure 5 shows a summary plot from the cross-section measurements made by ATLAS with the 2010 and 2011 datasets. The results show good agreement with the Standard Model predictions.

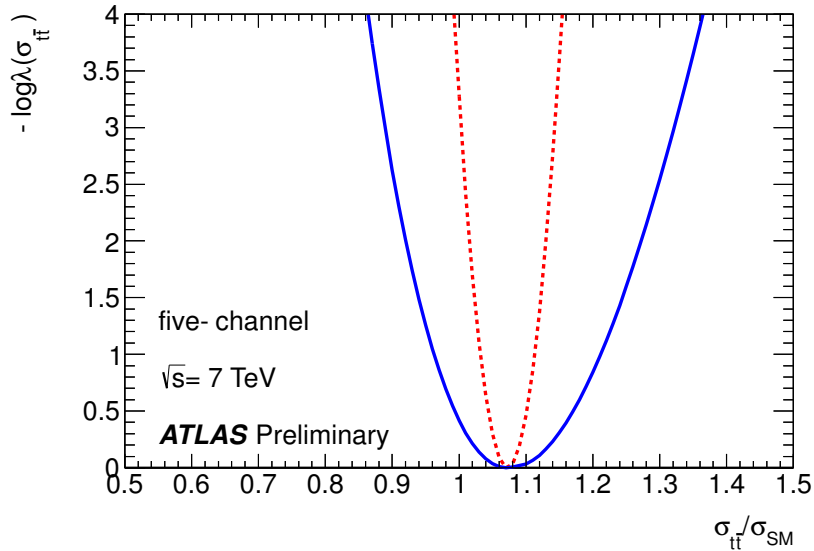


Figure 3: Graph of  $-\log \lambda(\sigma_{t\bar{t}})$  vs.  $\sigma_{t\bar{t}}/\sigma_{SM}$  with (blue, solid) and without (red, dashed) systematic uncertainties for the five-channel combined fit.

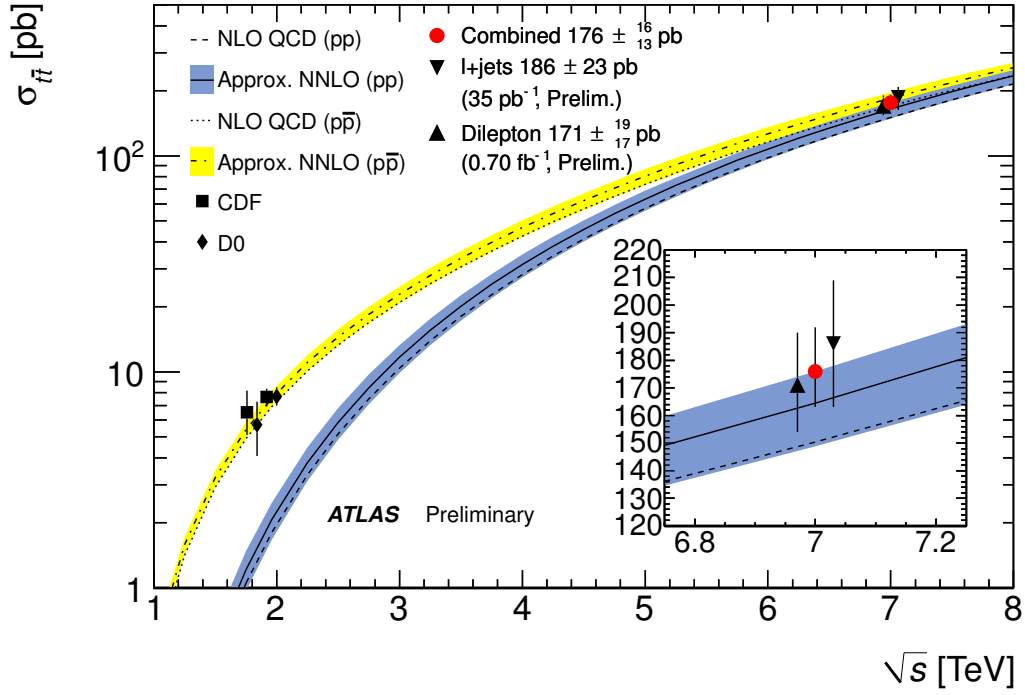


Figure 4: Dependence of  $\sigma_{t\bar{t}}$  on  $\sqrt{s}$  from theoretical predictions based on a top mass of 172.5 GeV together with the dilepton, single lepton, and combined measurements from ATLAS in this note. Uncertainties on measurements are shown as vertical bars and include statistical, systematic, and luminosity contributions. Results obtained with the Tevatron are also shown. Measurements made at the same center-of-mass energy are slightly offset for clarity.



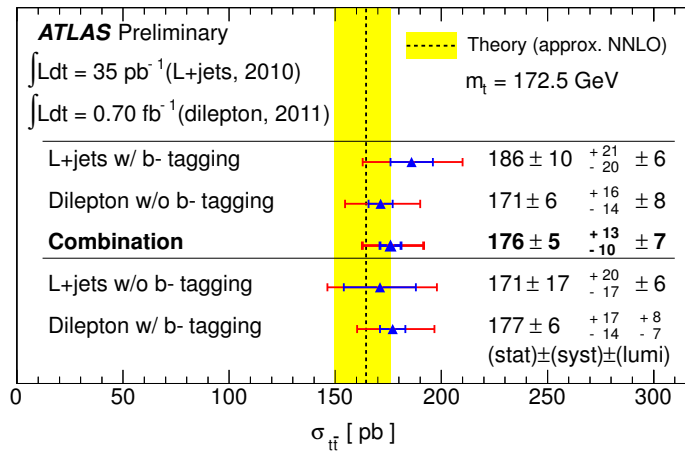


Figure 5: The measured value of  $\sigma_{t\bar{t}}$  in the single-lepton with  $b$ -tagging channel, the dilepton without  $b$ -tagging channel, and the combination of these two channels, including error bars for both statistical uncertainties only (blue) and including systematic uncertainties (red). For comparison, cross-section measurements using single-lepton without  $b$ -tagging and dilepton with  $b$ -tagging channels are shown. However these are not used in the five-channel combination. The approximate NNLO prediction with its error (yellow) is also shown.

## References

- [1] S. Moch and P. Uwer, “Theoretical status and prospects for top-quark pair production at hadron colliders”, *Phys. Rev. D* 78 (2008) 034003;  
U. Langenfeld, S. Moch, and P. Uwer, “New results for  $t\bar{t}$  production at hadron colliders”, DESY-09-104, SFB/CPP-09-61, HU-EP-09/31.
- [2] ATLAS Collaboration, “Measurement of the top quark-pair production cross section with ATLAS in pp collisions at  $\sqrt{s} = 7$  TeV”, *Eur. Phys. J. C* 71 (2011) 1577.
- [3] M. Aliev, H. Lacker, U. Langenfeld, S. Moch, and P. Uwer, “*HATHOR*, HAdronic Top and Heavy quarks crOss section calculator”, *Comput. Phys. Commun.* 182 (2011) 10341046, arXiv:1007.1327 [hep-ph].
- [4] ATLAS Collaboration, “Measurement of the top quark-pair cross-section with ATLAS in pp collisions at  $\sqrt{s} = 7$  TeV in the single-lepton channel using b-tagging,” ATLAS-CONF-2011-035, cdsweb.cern.ch/record/1337785.
- [5] ATLAS Collaboration, “Measurement of the top quark pair production cross section in pp collisions at  $\sqrt{s} = 7$  TeV in dilepton final states with ATLAS,” ATLAS-CONF-2011-100.
- [6] ATLAS Collaboration, “Updated Luminosity Determination in pp Collisions at  $\sqrt{s} = 7$  TeV using the ATLAS Detector”, ATLAS-CONF-2011-011, cdsweb.cern.ch/record/1334563.
- [7] F. James, “MINUIT Reference Manual”, CERN Program Library Writeup D506.
- [8] W. Verkerke, D. P. Kirkby, “The RooFit toolkit for data modeling,” in the proceedings of CHEP 2003, California, USA [physics/0306116].
- [9] L. Moneta, K. Belasco, K. Cranmer, A. Lazzaro, D. Piparo, G. Schott, W. Verkerke, M. Wolf *et al.*, “The RooStats Project,” in the proceedings of ACAT 2010, Jaipur, India (2010) [arXiv:1009.1003].
- [10] ATLAS Collaboration, “Performance of Impact Parameter-Based b-tagging Algorithms with the ATLAS Detector using Proton-Proton Collisions at  $\sqrt{s} = 7$  TeV,” ATLAS-CONF-2010-091, cdsweb.cern.ch/record/1299106.
- [11] CMS Collaboration “Combination of top pair production cross sections in pp collisions at  $\sqrt{s} = 7$  TeV and comparisons with theory”, CMS-PAS-TOP-11-001, cdsweb.cern.ch/record/1336491.
- [12] CDF Collaboration “Combination of CDF top quark pair production cross-section measurements with up to  $4.6 fb^{-1}$ ”, Conf Note 9913.
- [13] ATLAS Collaboration, “Top Quark Pair Production Cross-section Measurements in ATLAS in the Single Lepton+Jets Channel without b-tagging,” ATLAS-CONF-2011-023, cdsweb.cern.ch/record/1336753.